Colloids and Surfaces B: Biointerfaces 190 (2020) 110888

Contents lists available at ScienceDirect

Colloids and Surfaces B: Biointerfaces

journal homepage: www.elsevier.com/locate/colsurfb

A novel BSA immobilizing manner on modified titanium surface ameliorates osteoblast performance

O.P. Gomes[a,*], G.S. Feltran[b], M.R. Ferreira[b], C.S. Albano[a,b], W.F. Zambuzzi[b], P.N. Lisboa-Filho[a]

[a] São Paulo State University, UNESP, School of Sciences, Department of Physics, Bauru, São Paulo, Brazil
[b] São Paulo State University, UNESP, Institute of Biosciences of Botucatu, Department of Chemistry and Biochemistry, Botucatu, São Paulo, Brazil

ARTICLE INFO

Keywords:
Surface functionalization
Biomaterials
Biological interaction
Thin films

ABSTRACT

Surface modification of medical and dental devices, to improve their biocorrosion resistance and biocompatibility, can be achieved with the multidisciplinary field of biomaterials. Nanostructured titanium dioxide (TiO_2) has been employed as surface modifier of titanium-based biomaterials because it can prevent the failure of the devices due to wear mechanisms. Moreover, this oxide surface is mostly terminated by hydroxyl groups (-OH) that can be directly functionalized with biomolecules to improve the biocompatibility of these devices. We explored the influence of 3-aminopropyltrimethoxysilane (APTMS) molecules as spacers in bovine serum albumin (BSA) protein immobilization on the physically hydroxylated surfaces of rutile phase TiO_2 films grown by reactive Radio Frequency (RF) magnetron sputtering. X-ray Photoelectron Spectroscopy (XPS) was used to examine the adsorption of BSA and APTMS on the hydroxylated surface of TiO_2 thin films. For biological tests, BSA was directly immobilized on the film surface and on the APTMS monolayer. Biological analysis found better osteoblast performance considering gene markers related to cell adhesion after interacting directly with the surface modified by the immobilization of BSA, especially on the surface where this protein was immobilized by APTMS. Additionally, we addressed the relevance of this biointerfaces on extracellular matrix remodeling by zymography analysis. Altogether, our data provides new insights about the cellular and molecular mechanisms covering the improved osteoblastic response of the proposed surface modification.

1. Introduction

Implants used in dentistry or orthopedic surgery are mostly produced from metallic materials. Pure titanium and its alloys are the most commonly used due to their appropriate mechanical properties. However, these materials often do not have adequate biocompatibility, as they do not facilitate integration with the tissues adjacent to the implanted area [1]. Biocompatibility involves the interaction between a biomaterial and living tissue [2], and biocompatible materials need to have some pre-defined requirements, such as appropriate mechanical loading (strength, rigidity, surface hardness, and wear resistance), noninflammatory response, nontoxic, and does not provoke allergic or immunologic reactions [3–8]. Among the strategies to ameliorate biological performance of these materials, surface modification may provide biocorrosion resistance and even promote bioactivity by enhancing the interaction of the implant surface with specific proteins. Interaction with proteins is the initial process that occurs between the biological environment and the implant surface, and this dictates subsequent interactions, such as cell adhesion [9].

Titanium dioxide has been used in several studies as a surface modifier because of its high hardness, high dielectric constant, and chemical stability [10,11]. Coatings with adequate mechanical properties are important for orthopedic and dental implants because the failure of the materials is usually the result of different wear mechanisms [1]. Ochsenbein et al. [12] observed that the titanium oxide layer had satisfactory cell adhesion and proliferation. However, with the long-term exposure to a biological environment, the fine native oxide (5–6 nm) failed to protect the material from corrosion. On the other hand, a thicker and homogeneous titanium dioxide coating (100 nm) significantly increased the long-term biocorrosion resistance of Ti, exhibiting a similar cellular response. In addition, Werner et al. [13] found that the native oxide layer was generally less hemocompatible than a thicker and more homogeneous layer of TiO_2.

Among the various thin film deposition approaches, the Radio Frequency (RF) magnetron sputtering deposition technique provides precise control over the composition and surface morphology by adjusting the deposition parameters [14]. The properties of TiO_2 strongly depend on the microstructure and the crystallographic phase (rutile,

* Corresponding author.
E-mail address: orisson.gomes@unesp.br (O.P. Gomes).

https://doi.org/10.1016/j.colsurfb.2020.110888
Received 17 October 2019; Received in revised form 25 January 2020; Accepted 19 February 2020
Available online 20 February 2020

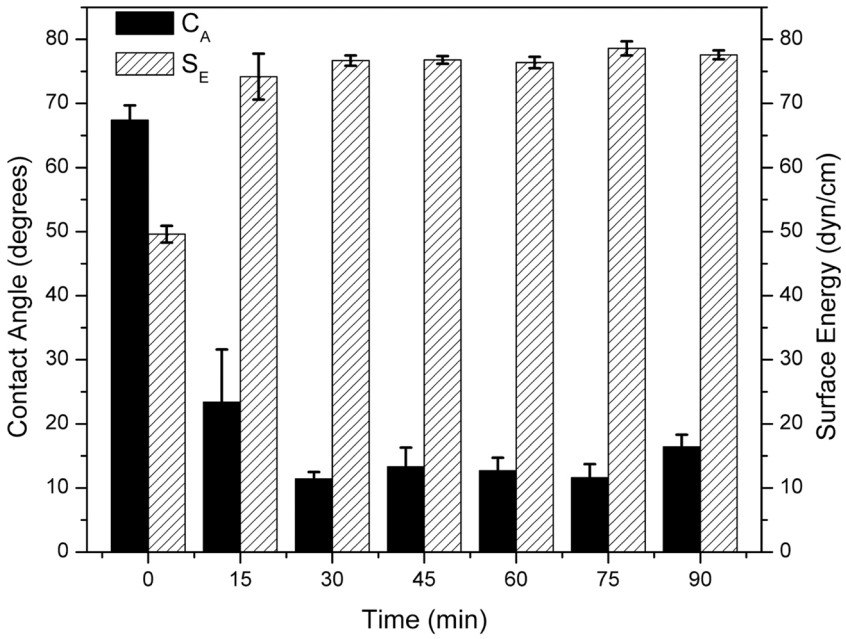

Fig. 1. Contact angle and surface energy values for samples exposed in UV lamp at times t = 0, 15, 30, 45, 60, 75, and 90 min. In the legend, C_A refers to the contact angle and S_E refers to the surface energy.

anatase, or brookite), where the rutile phase presents high mechanical resistance, while the anatase phase has high photocatalytic activity [15,16]. Thus, this technique may produce films with high uniformity, good adhesion, and high hardness, which are all desirable characteristics for use in biomedical implants.

Chemically, the surface of this oxide (TiO_2) is mainly terminated by -OH groups, which can be readily functionalized by various molecules containing different functional groups such as silanes, carboxylic acids, and other derivatives including esters, acid chlorides, and carboxylate salts, by forming self-assembled monolayers (SAMs) on the oxide surface [17]. The hydroxyl groups on the surface of the oxide tends to form covalent bonds with a specific functional group of the organic compound, through condensation reactions [18,19]. These -OH groups and the electrical charges formed by dissociation play an important role in binding to polymers, proteins, and immobilization of organic molecules [17]. Studies have suggested that the amount of -OH groups on the TiO_2 surface influences the photocatalytic activity and the hydrophilicity of the film [20].

The adsorption of the proteins in the blood and proteoglycans on the surface of the implants is important for the interaction of implants with the surrounding tissue [21] and determines the subsequent stages of cell adhesion and proliferation [22,23]. Therefore, the immobilization of certain types of protein on the surface of biomaterials might ameliorate their biocompatibility and performance. To ensure cell adhesion and subsequent proliferative phenotype, the most used proteins are those that naturally interact with connective tissue cells, such as osteoblasts, and with plasma constituents, such as platelets and leukocytes [24]. Among them, albumin is recognized as a major circulating component of blood [25]. It is expected that when immobilized on the surface of the material, this protein could play a role in bioactivity and promote improvement in the corrosion resistance of the implant [26–28].

Naturally after implanting, proteins adsorb on the surface of the metal oxide directly or through binding agents, considering mostly the properties of their amino-acids, which can simultaneously present hydrophobic, polar uncharged, and polar regions loaded on their surface. Thus, the interactions might be due to hydrophilicity, hydrophobicity, ionic interactions, or the formation of covalent bonds with a specific functional group of the molecule [29,30]. Often, the use of binding agents in the process of protein immobilization might provide greater steric freedom to the protein, which in turn allows a greater specific activity. In molecules used as spacers, one of the organic ligand groups interacts with the surface of the oxide and the other organic ligand group interacts with the protein [30].

Based on this background, the current study evaluated the influence of 3-aminopropyltrimethoxysilane [$H_2N(CH_2)_3Si(OCH_3)_3$] (APTMS) molecules used as spacers for bovine serum albumin (BSA) protein immobilization process on the physically hydroxylated surfaces of rutile phase TiO_2 films grown by reactive RF magnetron sputtering on titanium substrates. The modified surfaces were biologically evaluated via cytotoxicity assay and molecular analysis of specific gene activation using qPCR technology. The biological analysis of the modified surfaces was made by direct contact with pre-osteoblasts (MC3T3-E1, subclone 4, cell line). In brief, our data indicated improved osteoblastic response of the surface modified by BSA immobilized in the presence of APTMS spacer molecule and this opens new perspectives to be applied in bone related surgical processes. However, this set of data is for preclinical protocols.

2. Material and methods

Commercially pure titanium (cp-Ti) grade 4 was used as substrates due to its extensive use in various kinds of implants [31]. The procedures used to uniformize the substrate surfaces by wet sanding and the growth parameters of rutile phase TiO_2 films via reactive RF magnetron sputtering were described in a previous work [32]. The XPS measurements were performed on a Kratos spectrometer (AXIS-165) using a monochromatic Al Kα X-ray source. Each sample was analyzed at a 54.7° angle, defined as the emission angle relative to the surface. The energy resolution was 0.45 eV. The pass spectrum energy of the spectra was 80 eV and the individual high-resolution spectra was 20 eV. To correct for any charging effect, the binding energy of the Ti $2p_{3/2}$ peak was normalized to 458.8 eV. The CasaXPS computational package was used for the chemical study and analysis of the functionalized sample surfaces.

2.1. Hydroxylation test

After the growth of TiO_2 films, a set of samples was submitted to physical hydroxylation tests to find the best exposure time for higher hydrophilicity and surface energy for the subsequent functionalization procedure. This procedure consisted in exposing samples to ultraviolet light using an assembly that we built containing a UV lamp (P = 8 W, λ = 256 nm). The functionalization was performed after hydroxylation of TiO_2 surfaces by UV exposition for 30 min, which was the best time (Fig. 1). The contact angle and surface energy measurements of this work were obtained by the Ramé-Hart 100-00 goniometer. Water and diiodomethane were used as the polar and non-polar liquids, respectively.

2.2. APTMS functionalization

The procedure consisted of immersing hydroxylated TiO_2 surfaces in APTMS solution (Sigma-Aldrich, 97 %) with anhydrous ethanol at a concentration of 3 mM for one hour. After this period, they were rinsed with anhydrous ethanol. This washing procedure was performed three times to remove unbound molecules.

2.3. BSA functionalization

The samples were immersed in BSA solution (Sigma-Aldrich, ≥96 %) in PBS at a concentration of 0.40 mg/mL, for 6 h. Then, they were rinsed with Milli-Q water to remove the unbound proteins and the PBS salts [33,34]. This washing procedure was performed three times.

2.4. Cell culture

Pre-osteoblastic MC3T3-E1 cell line, obtained from mice, were cultured in α-MEM (minimal essential medium with alpha modification) supplemented with 10 % fetal bovine serum (FBS) and 1% antibiotic (penicillin and streptomycin) (NUTRICEL, Campinas, SP, Brazil). The cultured cells were maintained in an incubator at 37 °C and atmosphere of 5% CO_2 for 3 h and 72 h. Sub-confluent passages were trypsinized and used in all experiments of this study.

2.5. MTT assay

The MTT solution was prepared from the salt of the compound (Sigma-Aldrich, ≥ 97.5 %) in serum-free (α-MEM) medium at a concentration of 1 mg of the salt for each 1 ml of serum.

The cultured cells were seeded on the surfaces of the four groups (Ti, TiO_2, TiO_2 + BSA and TiO_2 + APTMS + BSA) in 24-well plates (5.5×10^4 cells/ml) and maintained in the incubator for 3 h. After this period, the samples were transferred to a new 24-well plate, and the MTT solution was added to each well. The samples were then placed back into the incubator for 3 h. Next the medium containing the MTT solution was removed and absolute alcohol was added in each well for solubilization of the blue dye formed by the viable cells. Finally, this solubilized medium was transferred to a 96 well plate, using an extra column (alcohol only) to serve as reference. This 96-well plate was taken to the microplate reader (SYNERGY-HTX, Biotek, USA) and the absorbance of the groups was measured at the wavelength of 570 nm [35]. In this assay, an experimental n equal to 9 was used for each group.

2.6. Cell adhesion assay

The Violet Crystal Solution was prepared from the powder of the compound (Sigma-Aldrich, ≥ 90 %) at a concentration of 0.1 % by weight (g) of the powder relative to the volume (ml) of distilled water (e.g. 0.04 g of violet crystal in 40 mL of distilled water).

The cultured cells were seeded on the surfaces of the four groups (Ti, TiO_2, TiO_2 + BSA, and TiO_2 + APTMS + BSA) in 24-well plates (5.5×10^4 cells/ml) and maintained in the incubator for 3 h. Then, the samples were transferred to a new 24 well plate and the wells containing the samples were washed twice with warm PBS. After washing, the cells on the samples were fixed in absolute ethanol solution with acetic acid (3:1; v/v) in each well, and the plate was maintained for 10 min at room temperature. Next the solution was aspirated, and the violet crystal solution was added to each well. After a 10 min wait, the excess dye was removed by decantation and washed twice with distilled water and the dye was extracted with 10 % (v/v) acetic acid. Finally, the stained medium was transferred to a 96-well plate, using an extra column (with only 10 % acetic acid) to serve as reference. This 96-well plate was taken to the microplate reader (SYNERGY-HTX, Biotek, USA) and the absorbance of the groups was measured at the wavelength of 540 nm [36]. In this test, an experimental n equal to 9 was also used for each group.

2.7. Real-time polymerase chain reaction (qPCR)

Cells were cultured on the surfaces of the four groups for the time periods of 3 and 72 h (3 days). Total mRNA was extracted using the Ambion TRIzol Reagent kit (Life Sciences - Fisher Scientific, Waltham, MA, USA) and treated with DNase I (Invitrogen, Carlsbad, CA, USA). The cDNA synthesis was performed with the High Capacity cDNA Reverse Transcription Kit (Applied Biosystems, Foster City, CA, USA) according to the manufacturer's instructions. The reactions to study the expression pattern of genes involved in the adhesion process were performed in triplicate using SYBR Green Master Mix (q-PCR®, Promega) and specific primers related to cell adhesion, and the choice of them is discussed in session 3.2. To calculate the relative quantity, the comparative critical threshold method 2-ΔCt was employed. The results were expressed as mean ± standard deviation of 3 independent experiments with the genes GAPDH, β-actin, and 18S as internal controls. Primers and details are listed in Table 1.

2.8. Zymography

Given their involvement in a variety of physiological processes, which are explained in session 3.3, the proteolytic activities of the MMP-2 and MMP-9 were measured with respect to the gelatin-based zymography protocol for 3 and 72 h. After performing the direct contact experimental circuit with the four different surfaces (groups), the conditioned culture medium was collected and centrifuged at 14,000 rpm for 15 min to avoid cellular debris, and the protein concentration was determined by the method of Lowry [37]. Then, 150 µg of protein was applied to a 12 % polyacrylamide gel containing 4% of gelatin. The gelatinolytic activity of the proteins involved was determined by renaturating them using Triton X-100 in aqueous solution (2% w/v) for 40 min under stirring at 37 °C, and proteolysis buffer (Tris-$CaCl_2$) incubated for 18 h also at 37 °C. The gel was then stained with Coomassie Blue (0.05 % R-250 dye solution) for 3 h, after which time, the gel was washed in 30 % (v/v) methanol solution and 10 % (v/v) glacial acetic acid. The absence of staining was obtained in regions of the gel which had the gelatinolytic activity (bands) of MMP2 (~ 62 kDa) and MMP9 (~ 84 kDa). These bands were then subjected to densitometry analysis using the ImageJ software (Bethesda, MD, USA) [38] and the obtained pixel values transferred to the GraphPad Prism7 software (GraphPad Software Inc., San Diego, CA, USA) for statistical analysis.

2.9. Statistics

All the biological experiments were performed at least three times for better statistics, and the results were expressed as the mean ± standard deviation (SD). A one-way analysis of variance (ANOVA) was performed using the Tukey test for multiple comparisons with the

Table 1
Sequences of gene expression primers and PCR cycle conditions.

Gene (ID)	Primer	5′- 3′ Sequence	Reaction Conditions
GAPDH	Forward	**AGGCCGGTGCTGAGTATGTC**	95 °C - 15 s; 63 °C - 30 s; 72 °C - 30 s
(14433)	Reverse	**TGCCTGCTTC ACCACCTTCT**	
18S	Forward	**CGCTATCTGACTCGCTG**	95 °C - 15 s; 53 °C - 30 s; 72 °C - 30 s
(19791)	Reverse	**GGAAGGTTCTAGTCAGG**	
β-actin	Forward	**TCTTGGGTATGGAATCCTGTG**	95 °C - 15 s; 63 °C - 30 s; 72 °C - 30 s
(11461)	Reverse	**AGGTCTTTACGGATGTCAACG**	
Fak	Forward	**TCCACCAAAGAAACCACCTC**	95 °C - 15 s; 60 °C - 30 s; 72 °C - 30 s
(14083)	Reverse	**ACGGCTTGACACCCTCATT**	
Src	Forward	**TCGTGAGGGAGAGTGAGAC**	95 °C - 15 s; 60 °C - 30 s; 72 °C - 30 s
(17977)	Reverse	**GCGGGAGGTGATGTAGAAAC**	
Cofilin	Forward	**CAGACAAGGACTGCCGCTAT**	95 °C - 15 s; 60 °C - 30 s; 72 °C - 30 s
(12631)	Reverse	**TTGCTCTTGAGGGGTGCATT**	
Integrin-β1	Forward	**CTGATTGGCTGGAGGAATGT**	95 °C - 15 s; 60 °C - 30 s; 72 °C - 30 s
(16412)	Reverse	**TGAGCAATTGAAGGATAATCATAG**	
Integrin-α1	Forward	**CTGATTGGCTGGAGGAATGT**	95 °C - 15 s; 60 °C - 30 s; 72 °C - 30 s
(109700)	Reverse	**TGAGCAATTGAAGGATAATCATAG**	

GraphPad Prism7 software (GraphPad Software Inc., San Diego, CA, USA) to evaluate whether different treated surfaces influenced the adhesion. Differences between the means were considered significant when $P < 0.05$ (*) or highly significant when $P < 0.001$ (***) (****).

3. Results and discussion

The urgent need to improve biocompatibility of titanium-based alloys should focus mainly on patients' recovery speed. Over the last several years, we have concentrated on a proposed set of methodologies to better address the biointerfaces of biomaterials, considering cellular and molecular mechanism governing the behavior of cell interaction on biomaterial surfaces [39]. This study proposes a new approach that optimizes osteoblastic response of the biofunctionalized surface of titanium employing biological analysis to support the potential of this material for evaluation in preclinical studies.

3.1. Surface characterization

Fig. 1 provides the mean values of contact angle (C_A) and surface energy (S_E) for different samples exposed to UV radiation at times t = 0, 15, 30, 45, 60, 75, and 90 min. For each time, three measurements of contact angle were conducted with water (as polar liquid) and diiodomethane (as apolar liquid). The surface energy values were then calculated from these measurements. The lowest contact angles were for times t = 35 and 75 min (11.4° and 11.6°, respectively). The highest surface energy values were also for these times (76.7 dyn/cm and 78.6 dyn/cm, respectively). The changes were very noticeable between the samples without exposure (t = 0) and the samples exposed to UV radiation. The surface changed from intermediate (67.4°) to hydrophilic (values below 30°), with a significant increase in surface energy. The photocatalytic property of TiO_2, described by Hashimoto, Irie, and Fujishima [40], results in a higher number of hydroxyls available on the surface after exposure to UV radiation. The contact angle and surface energy values for the 30 and 75 min were close, but the standard deviation for the 75 min time was higher; therefore, we choose 30 min of exposure time as the standard for the preparation and subsequent functionalization of the samples

The reason for doing this initial study is that surface energy can indicate the ability of a given surface to interact spontaneously with other materials to form new bonds. Therefore, the results presented were satisfactory, since higher surface energy values are desirable for better interaction with APTMS molecule and bovine serum albumin (BSA) protein. In addition, according to Hallab et al. [41], they demonstrated a correlation between surface energy, cell adhesion capacity, and subsequent cell proliferation. For wettability, hydrophilic surfaces exhibit greater cell adhesion and proliferation capacity [42–44].

The XPS technique was used to analyze the surface chemistry of the studied groups, as well as confirm the spatial conformation of APTMS molecule, to evaluate the effectiveness of the functionalization process. In the high-resolution spectra, the values of residual standard deviation (RSD) were indicated as the quality factor of the realized fittings.

Fig. 2a–c presents the high-resolution spectra after the functionalization procedure with APTMS molecules. The O 1s high-resolution spectrum (Fig. 2a) contains three contributions. The contribution at 529.48 eV refers to the O-Ti-O bond of titanium dioxide, and the contribution at 530.15 eV describes the hydroxyl groups. The third contribution, at 531.90 eV, refers to the Ti-O-Si bond and indicates the adhesion of the APTMS molecules on the surface of the titanium dioxide by the silane group. The binding between the APTMS molecules by the silane group and the substrate stabilizes the monolayer formed over the

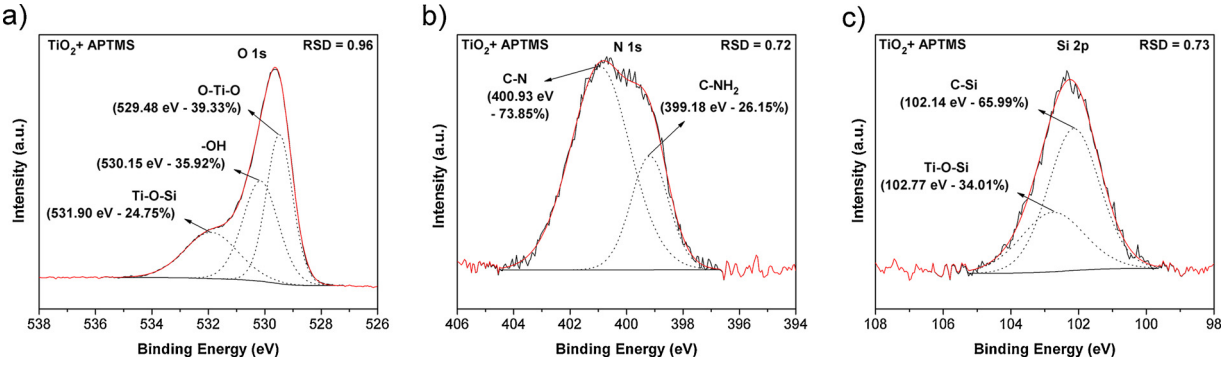

Fig. 2. a) High resolution spectrum O 1s, b) high resolution spectrum N 1s, c) high resolution spectrum Si 2p of TiO_2 sample after APTMS functionalization process.

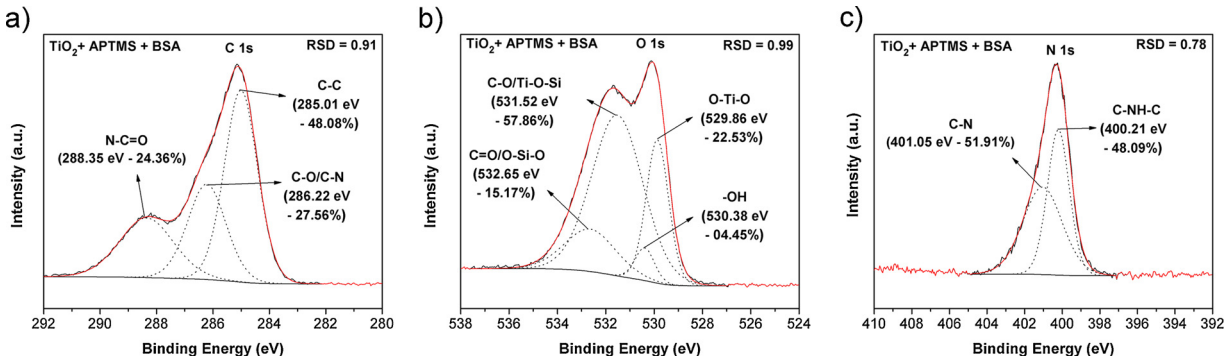

Fig. 3. a) High resolution spectrum C 1s, b) High resolution spectrum O 1s, and c) High resolution spectrum N 1s of the TiO_2 sample after APTMS functionalization process and subsequent BSA.

TiO_2 surface and this reaction is known as silanization. This result is consistent with those presented in the literature, where normally the silanization occurs on hydroxylated surfaces [19].

In the N 1s high-resolution spectrum (Fig. 2b), the two contributions refer to APTMS molecule, where one indicates the amine group (NH_2) in 399.18 eV, and another refers to the C—N bond in 400.93 eV. The lack of Ti-N type contribution suggests that APTMS molecule displays a preferential interaction with the TiO_2 surface by the silane group, leaving the amine group free [45]. In addition, a contribution of the Ti-O-Si bond in the Si 2p high-resolution spectrum (Fig. 2c) in 102.77 eV was detected, and a further contribution was also observed in 102.14 eV, related to the C-Si bond of the APTMS molecule.

Fig. 3a–c shows the high-resolution spectra of the TiO_2 sample after the functionalization procedure with APTMS, followed by the functionalization process with the BSA protein, respectively. The APTMS molecule was used as a spacer in the immobilization process of BSA on the TiO_2 surface. As the BSA molecules are much larger than the APTMS molecules and the composition of the elements of both are similar, the high-resolution spectra mostly present data related to the chemical bonds of the BSA molecules and the surface of the TiO_2. In the C 1s high-resolution spectrum (Fig. 3a), three contributions can be observed, one at 285.01 eV referring to C—C bond, another at 286.22 eV referring to C—O/C-N bond, and the other at 288.35 eV referring to N-C=O bond; these contributions are related to the bonds present in BSA, except C—N, which is also present in APTMS. The O 1s high resolution spectrum (Fig. 3b) shows four contributions, one at 532.65 eV referring to the C=O or O-Si-O bond, at 531.52 eV referring to the bond C—O or TO-Si, an O-Ti-O contribution at 529.86 eV, and another concerning the terminal hydroxyls (530.38 eV) present on the surface of the oxide. Two contributions are visible in the N 1s high-resolution spectrum (Fig. 3c), one referring to the C—N bond (401.55 eV) and the other to the amine group (399.84 eV). The APTMS molecules attached to the TiO_2 surface by the silane group; thus, the results suggest that BSA bounded to the amine group of APTMS molecules. However, given the size and complexity of proteins in general, the exact region that the BSA bonded with APTMS cannot be determined. Previous results suggest the formation of APTMS monolayer on TiO_2 surface, and the washing process after immersion of the substrates in APTMS and BSA solutions ensures that the unbound molecules were removed. All of these procedures were performed to guarantee that the BSA molecules indeed bonded to the TiO_2 surface with the APTMS molecules (spacer).

3.2. Modified titanium surfaces drive osteoblast adhesion and improved biocompatibility

To address the biological response of this proposed surface, we used pre-osteoblast cells, because the focus of this work is to study the biological performance of a bone implant candidate (orthopedic/dental) [46]. First, cellular and molecular mechanisms were analyzed. Fig. 4 illustrates the cell viability and adhesion data performed by MTT and Violet Crystal, respectively. The results obtained by the cellular viability assay (Fig. 4a) indicates significantly higher mitochondrial activity of pre-osteoblasts for all groups, especially responding to TiO_2 + APTMS + BSA group. The cell adhesion assay (Fig. 4b) presented a very similar profile for cell viability, where a higher number of viable cells were found in response to TiO_2 + APTMS + BSA surfaces. The higher cell adhesion on BSA-modified surfaces might be due to the capacity of integrins to crosslink the intracellular compartment with organic molecules in the extracellular microenvironment [47]. The date from both colorimetric assays corroborates with others when the titanium surface was modified by the growth of the TiO_2 film [48,49]. In addition, they suggest improved osteoblastic response of the TiO_2 surface modified with BSA, especially when immobilized in the presence of the spacer APTMS molecule. The molecular machinery supporting this behavior is presented later in this study.

Previously, we obtained better attaching behavior of osteoblasts on BSA-modified surfaces, and it was shown to be under a specific molecular machinery. Thus, Fig. 5 presents the genes related to cell adhesion. Importantly, the better performance of osteoblast adhering on the BSA-modified surfaces is guaranteed by the higher activation of α1 and β1 integrins (approximately 3-fold-changes and 60-fold changes increased, respectively; Fig. 5a,b), which are responsible to modulate cell adhesion on organic surfaces. The cell adhesion process is regulated by intracellular mechanisms upon activation of integrins, which are heterodimeric transmembrane receptor proteins (α and β subunits) belonging to the group of cell adhesion molecules (CAMs). These proteins are intermediates in the communication between the cellular cytoskeleton and plasma proteins or the cell matrix through cell-to-cell adhesion through interactions with other membrane proteins. In addition to the adhesion function, these proteins are also recognized as signaling molecules able to transduce messages by classical signaling pathways, leading to the activation of FAK and Src intracellularly, and culminating with the phosphorylation of cofilin [50,51]. The activation of this set of genes is probably conserved, because a dynamic ECM remodeling occurs during osteoblast differentiation [52] that affects the adhesion and viability of the cells.

This set of gene encoding proteins related with cell adhesion and viability was evaluated in this study, and the data demonstrates a significant involvement of FAK (Fig. 5c), Src (Fig. 5d) and Cofilin (Fig. 5e) genes. It is important to mention the biphasic effect of Src in osteoblast, which participates positively with survival and proliferative signaling and negatively with differentiation-related signaling [53–55]. In sum, this molecular machinery triggered by TiO_2 + APTMS + BSA surfaces guarantees better performance of osteoblasts and partially explain the colorimetric assays illustrated Fig.4.

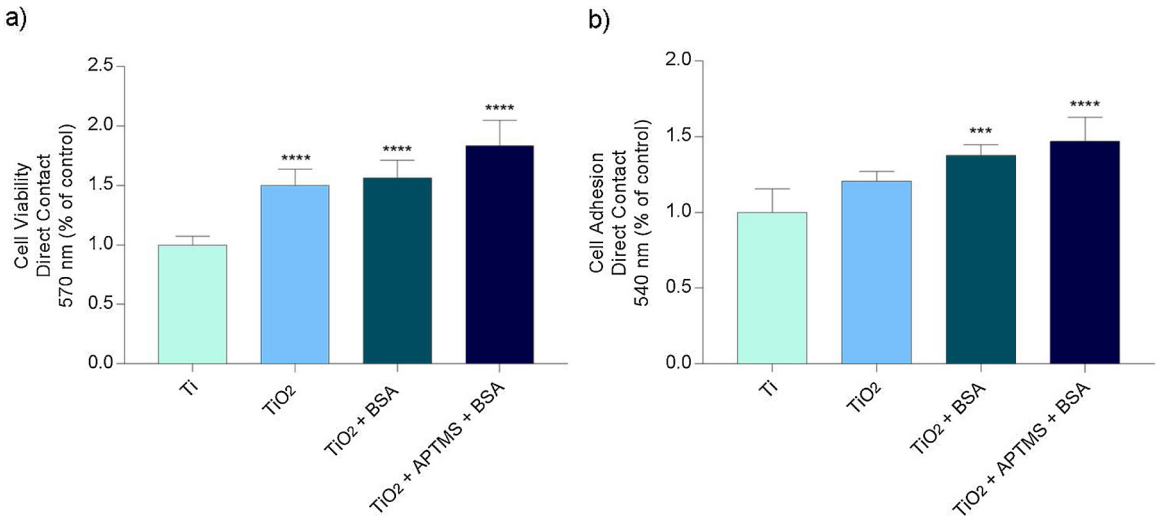

Fig. 4. The cytotoxic effects of the functionalized surfaces were evaluated for 3 h, through the mitochondrial dehydrogenase activity in the MTT assay and cellular adhesion from the crystal violet dye, representing the percentage of cellular viability of the pre-osteoblasts in (a) and the percentage of cells adhered in (b). Titanium presenting machined surfaces (Ti) was considered the control. The results are represented as the mean ± standard deviation from three independent experiments.

3.3. ECM remodeling in response to the BSA-modified surfaces

Extracellular matrix (ECM) remodeling is a necessary pre-requisite to cell adhesion [56] executed by MMPs. Thus, we have subjected the cells responding to the surfaces of this experimental design and the conditioned medium was harvested at 3 and 72 h to evaluate the activity of MMP2 and MMP9, as presented in Fig. 6. The data demonstrates significance in the higher activities of both MMP-2 and MMP-9 independent of 3 or 72 h responding to TiO_2 + APTMS + BSA surfaces. MMPs are zinc-dependent endopeptidases that process and degrade various extracellular proteins. They participate in a variety of physiological processes, such as angiogenesis, tissue repair, morphogenesis, stem cell mobilization, and wound healing [57,58]. Mizutani et al. [59] demonstrated that both MMP2 and MMP9 are involved in the osteoblastic differentiation process, indicating their participation in the formation and maturation of the ECM, and this data was completed in 2009 by Zambuzzi et al., who found strong involvement of TIMPs and RECK proteins in this process, suggesting finely modulated ECM remodeling during osteoblast differentiation (mainly responding to the osteogenic stimulus up to 28 days) [52]. Furthermore, during the osteoblast differentiation process, ECM remodeling might be understood as a preliminary mechanism to prepare the ECM for later

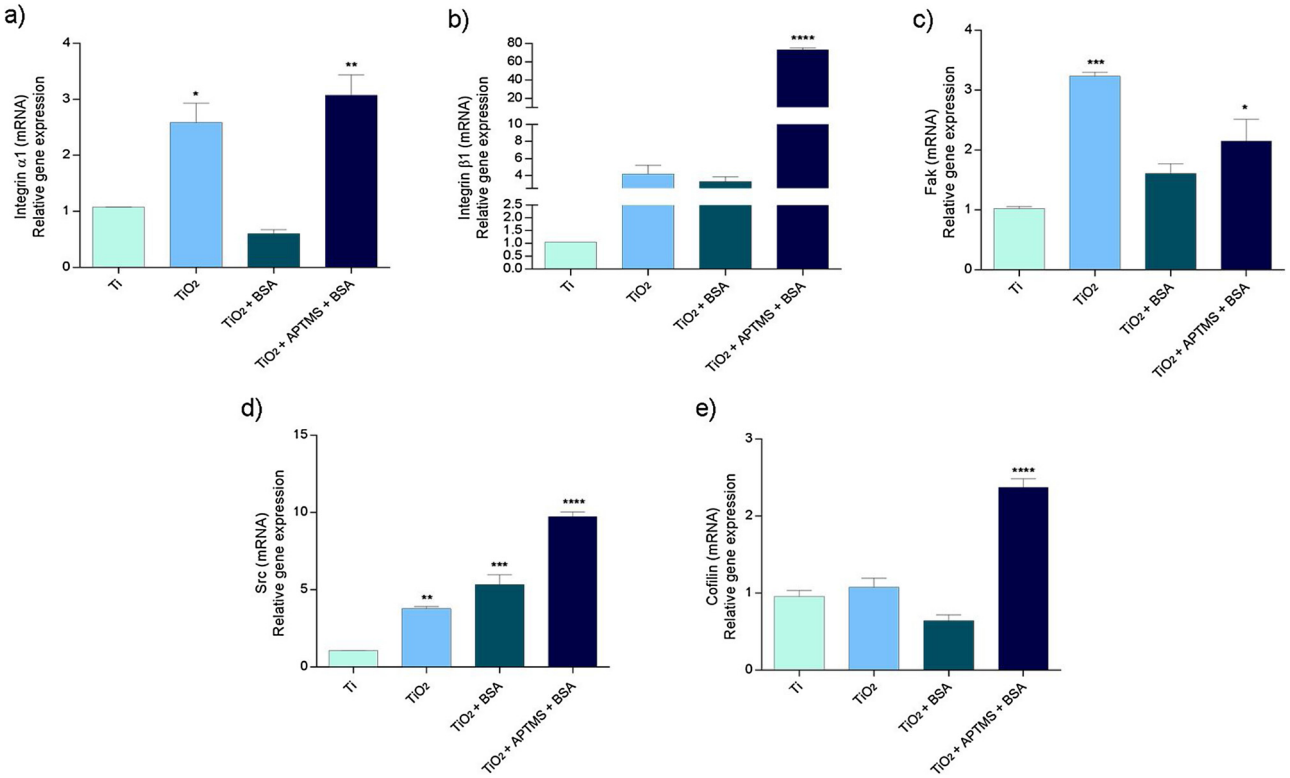

Fig. 5. The total mRNA was collected and adhesion-related [*Integrin α1* (a), *Integrin β1* (b), *Fak* (c), *Src* (d), and *Cofilin* (e)] genes were each analyzed. The results are represented as the mean ± standard deviation of three independent experiments. Titanium presenting machined surfaces (Ti) was considered the control.

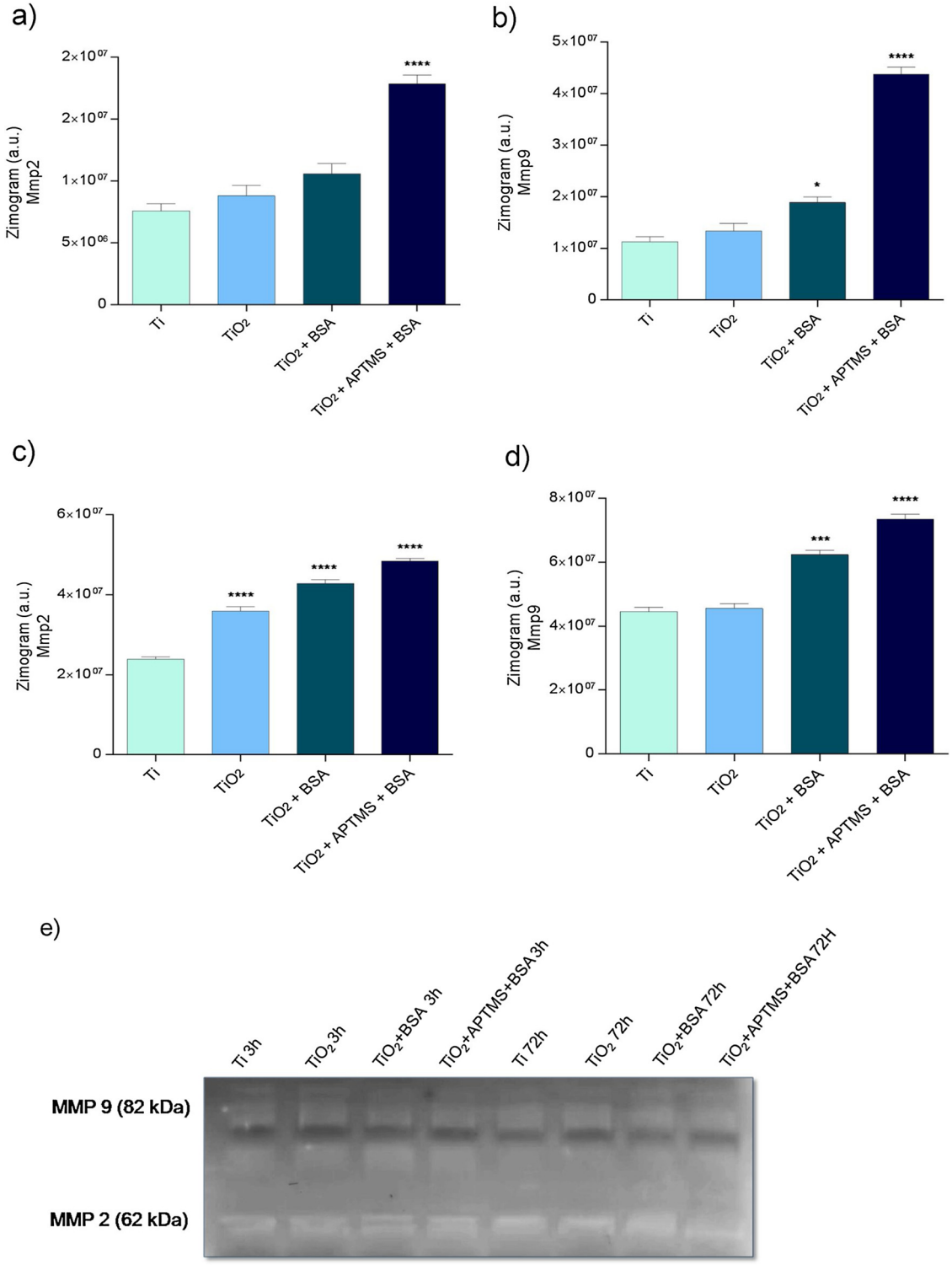

Fig. 6. Analysis of extracellular matrix remodeling for pre-osteoblasts after 3 h and 72 h. The activities of the MMPs were measured by the Zymography (e) assay and the analysis of these activities at 3 h [Mmp2 (a) and Mmp9 (b)] and 72 h [Mmp2 (c) and Mmp9 (d)] is presented. Titanium presenting machined surfaces (Ti) was considered the control. The results are represented as the mean ± standard deviation from three independent experiments.

mineralization.

4. Conclusions

Our data demonstrated that it was possible to reduce the contact angle of the film surfaces through the physical hydroxylation process and, consequently, to obtain surfaces with high wettability. According to chemical analysis, the XPS confirmed the adsorption of the APTMS molecules on the hydroxylated surfaces of TiO_2. Although the results obtained from the XPS do not provide exactly where the adhesion of the BSA occurred, strong evidence indicates that they bound to both the hydroxylated surface of TiO_2 and to the amine end group of the APTMS molecules used as spacers.

The biological performance of osteoblasts responding to TiO_2 +

APTMS + BSA surfaces shows it being an important way to improve the performance of BSA as a surface modifier agent and, thus, to biofunctionalize titanium surfaces to guarantee cell adhesion and viability. In summary, the modification of these surfaces with BSA protein, especially immobilized by APTMS molecule, makes the surface of titanium devices more suitable to osteoblast performance and it opens new perspectives to be applied in bone related surgical processes and these results indicate preclinical

CRediT authorship contribution statement

O.P. Gomes: Conceptualization, Methodology, Validation, Investigation, Writing - original draft, Writing - review & editing, Project administration, Visualization. **G.S. Feltran:** Investigation, Methodology, Formal analysis. **M.R. Ferreira:** Investigation, Methodology, Formal analysis. **C.S. Albano:** Investigation, Methodology. **W.F. Zambuzzi:** Conceptualization, Methodology, Resources. **P.N. Lisboa-Filho:** Conceptualization, Methodology, Supervision, Funding acquisition, Resources.

Acknowledgements

We would like to thank FAPESP (process number 2016/22186-7, 2014/20471-0, 2017/15035-5, and 2014/22689-3) and CEPID (2013/07296-2) for providing financial support.

References

[1] P. Silva-Bermudez, S.E. Rodil, An overview of protein adsorption on metal oxide coatings for biomedical implants, Surf. Coat. Technol. 233 (2013) 147–158.
[2] D.F. Williams, On the mechanisms of biocompatibility, Biomaterials 29 (20) (2008) 2941–2953.
[3] G.D.A.S. Feltran, F. Bezerra, C.J.D.A.C. Fernandes, M.R. Ferreira, W.F. Zambuzzi, Differential inflammatory landscape stimulus during titanium surfaces-obtained osteogenic phenotype, J. Biomed. Mater. Res. A. 107 (8) (2019) 1597–1604.
[4] C.J.C. Fernandes, F. Bezerra, M.R. Ferreira, A.F.C. Andrade, T.S. Pinto, W.F. Zambuzzi, Nano hydroxyapatite-blasted titanium surface creates a biointerface able to govern Src-dependent osteoblast metabolism as prerequisite to ECM remodeling, Colloids Surf. B Biointerfaces 163 (2018) 321–328.
[5] C.J. Da Costa Fernandes, F.J.B. Bezerra, B. De Campos Souza, M.A. Campos, W.F. Zambuzzi, Titanium-enriched medium drives low profile of ECM remodeling as a pre-requisite to pre-osteoblast viability and proliferative phenotype, J. Trace Elem. Med. Biol. 50 (2018) 339–346.
[6] M. Baroncelli, G.M. Fuhler, J. Van De Peppel, W.F. Zambuzzi, J.P. Van Leeuwen, B.C.J. Van Der Eerden, M.P. Peppelenbosch, Human mesenchymal stromal cells in adhesion to cell-derived extracellular matrix and titanium: comparative kinome profile analysis, J. Cell. Physiol. (2018) 1–13.
[7] M.C. Rossi, F.J.B. Bezerra, R.A. Silva, B.P. Crulhas, C.J.C. Fernandes, A.S. Nascimento, W.F. Zambuzzi, Titanium-released from dental implant enhances pre-osteoblast adhesion by ROS modulating crucial intracellular pathways, J. Biomed. Mater. Res. A. 105 (11) (2017) 2968–2976.
[8] W.F. Zambuzzi, E.A. Bonfante, R. Jimbo, M. Hayashi, M. Andersson, G. Alves, J.M. Granjeiro, Nanometer scale titanium surface texturing are detected by signaling pathways involving transient FAK and src activations, PLoS One 9 (7) (2014) 1–11.
[9] A. Kumari, S.K. Yadav, S.C. Yadav, Biodegradable polymeric nanoparticles based drug delivery systems, Colloids Surf. B Biointerfaces 75 (2010) 1–18.
[10] V. Zorba, X. Chen, S.S. Mao, Superhydrophilic TiO2 surface without photocatalytic activation, Appl. Phys. Lett. 96 (2010) 1–3.
[11] H.S. Chen, S.H. Huang, T.P. Perng, Highly transparent hard bio-coating synthesized by low temperature sol–gel process, Surf. Coat. Technol. 233 (2013) 140–146.
[12] A. Ochsenbein, et al., Osteoblast responses to different oxide coatings produced by the sol–gel process on titanium substrates, Acta Biomater. 4 (2008) 1506–1517.
[13] C. Werner, M.F. Maitz, C. Sperling, J. Mater. Chem. 17 (2007) 3376.
[14] D.L. Smith, Thin-Filme Deposition: Principles and Practice, 1 ed., McGRaw-Hill Education, 1995.
[15] J. Zhang, Y. Nosaka, Photocatalytic oxidation mechanism of methanol and the other reactants in irradiated TiO2 aqueous suspension investigated by OH radical detection, Appl. Catal. B Environ. 166–167 (2015) 32–36.
[16] Y. Kakuma, A.Y. Nosaka, Y. Nosaka, Difference in TiO2 Photocatalytic mechanism between rutile and anatase studied by the detection of active oxygen and surface species in water, Phys. Chem. Chem. Phys. 17 (2015) 1–8.
[17] T. Hanawa, A comprehensive review of techniques for biofunctionalization of titanium, J. Periodontal Implant Sci. 41 (2011) 263–272.
[18] J.C. Love, et al., Self-assembled tonolayers of thiolates on metals as a form of nanotechnology, Chem. Rev. 105 (2005) 1103–1169.
[19] S.P. Pujari, et al., Covalent surface modification of oxide surfaces, Angew. Chemie Int. Ed. 53 (n. 25) (2014) 6322–6356.
[20] M.E. Simonsen, Z. Li, E.G. Søgaard, Influence of the OH groups on the photocatalytic activity and photoinduced hydrophilicity of microwave assisted sol–gel TiO_2 film, Appl. Surf. Sci. 255 (2009) 8054–8062.
[21] K.E. Healy, P. Ducheyne, Hydration and preferential molecular adsorption on titanium in vitro, Biomaterials 13 (1992) 553–561.
[22] A. Abdolmaleki, S. Mallakpour, S. Borandeh, The use of novel biodegradable, optically active and nanostructured poly(amide-ester-imide) as a polymer matrix for preparation of modified ZnO based bionanocomposites, Mater. Res. Bull. 47 (5) (2012) 1123–1129.
[23] Y. Wang, et al., Research of protein adsorption on the different surface topography of the zinc oxide, Surf. Interface Anal. 47 (n. 2) (2015) 245–252.
[24] M.-C. Sin, et al., An intuitive thermal-induced surface zwitterionization for versatile, well-controlled haemocompatible organic and inorganic materials, Colloids Surf. B Biointerfaces 127 (2015) 54–64.
[25] A. Ameen, R. Short, C. Douglas, R. Johns, B. Ballet, A critical investigation of some of the procedures employed in the surgical use of titanium, J. Mater. Sci. Mater. Med. 7 (1996) 195–199.
[26] E. Anbazhagan, et al., Divalent ion encapsulated nano titania on Ti metal as a bioactive surface with enhanced protein adsorption, Colloids Surf. B Biointerfaces 143 (2016) 213–223.
[27] N.L. D'elia, et al., Albumin-mediated deposition of bone-like apatite onto nano-sized surfaces: effect of surface reactivity and interfacial hydration, J. Colloid Interface Sci. 494 (2017) 345–354.
[28] S. Höhn, et al., Albumin coatings by alternating current electrophoretic deposition for improving corrosion resistance and bioactivity of titanium implants, Mater. Sci. Eng. C Mater. Biol. Appl. 73 (2017) 798–807.
[29] T. Sjöström, et al., Titanium nanofeaturing for enhanced bioactivity of implanted orthopedic and dental devices, Nanomedicine 8 (2013) 89–104.
[30] M.S. Killian, Organic Modification of TiO_2 and Other Metal Oxides With SAMs and Proteins - a Surface Analytical Investigation. 2013. 233 f. Tese (Doutorado Em Engenharia), Faculdade de Engenharia, Friedrich-Alexander-Universität Erlangen-Nürnberg, Nürnberg, 2013.
[31] K. Cai, M. Müller, J. Bossert, A. Rechtenbach, K.D. Jandt, Surface structure and composition of flat titanium thin films as a function of film thickness and evaporation rate, Appl. Surf. Sci. 250 (2005) 252–267.
[32] O.P. Gomes, N.F. Azevedo Neto, E.S. Bronze-Uhle, L.D. Trino, C.M. dos Santos, J.H.D. da Silva, P.N. Lisboa-Filho, 3-Mercaptopropionic acid functionalization of titanium dioxide thin films, Mater. Chem. Phys. 223 (2019) 32–38.
[33] M. Advincula, X. Fan, J. Lemons, R. Advincula, Surface modification of surface sol–gel derived titanium oxide films by self-assembled monolayers (SAMs) and nonspecific protein adsorption studies, Colloids Surf. B Biointerfaces 42 (2005) 29–43.
[34] M.C. Martins, B.D. Ratner, M.A. Barbosa, Protein adsorption on mixtures of hydroxyland methylterminated alkanethiols self-assembled monolayers, J. Biomed. Mater. Res. A. 67 (2003) 158–171.
[35] T. Mosmann, Rapid colorimetric assay for cellular growth and survival: application to proliferation and cytotoxicity assays, J. Immunol. Methods 65 (1983) 55–63.
[36] F. Bezerra, M.R. Ferreira, G.N. Fontes, C.J. Da Costa Fernandes, D.C. Andia, N.C. Cruz, R.A. Da Silva, W.F. Zambuzzi, Nano hydroxyapatite-blasted titanium surface affects pre-osteoblast morphology by modulating critical intracellular pathways, Biotechnol. Bioeng. 118 (8) (2017) 1888–1898.
[37] E.F. Hartree, Determination of protein: a modification of the lowry method that gives a linear photometric response, Anal. Biochem. 48 (2) (1972) 422–427.
[38] V. Lefebvre, C. Peeters-Joris, G. Vaes, Production of gelatin-degrading matrix metalloproteinases ('type IV collagenases') and inhibitors by articular chondrocytes during their dedifferentiation by serial subcultures and under stimulation by interleukin-1 and tumor necrosis factor alpha, Biochim. Biophys. Acta. 1094 (1) (1991) 8–18.
[39] S. Gemini-Piperni, E.R. Takamori, S.C. Sartoretto, K.B. Paiva, J.M. Granjeiro, R.C. De Oliveira, W.F. Zambuzzi, Cellular behavior as a dynamic field for exploring bone bioengineering: a closer look at cell-biomaterial interface, Arch. Biochem. Biophys. 561 (2014) 88–98.
[40] K. Hashimoto, H. Irie, A. Fujishima, Tio_2 photocatalysis: a historical overview and future prospects, J. Appl. Phys. 44 (2005) 8269–8285.
[41] N. Hallab, K. Bundy, K. O'connor, R.L. Moses, J.J. Jacobs, Evaluation of metallic and polymeric biomaterial surface energy and surface roughness characteristics for directed cell adhesion, Tissue Eng. 71 (2001) 55–71.
[42] T.G. Ruardy, J.M. Schakenraad, H.C. Van Der Mei, H.J. Busscher, Adhesion and spreading of human skin fibroblasts on physocochemically characterized gradient surfaces, J. Biomed. Mater. Res. 29 (1995) 1415–1423.
[43] A. Georgi, F. Grinnel, T. Groth, Studies on the biocompatibility of materials: fibroblast reorganisation of substratum-bound fibronectin on surfaces varying in wettability, J. Biomed. Mater. Res. 30 (1996) 385–391.
[44] K. Webb, V. Hlady, P.A. Tresco, Relative importance of surface wettabillity and charged functional groups on NIH 3T3 fibroblasts attachment, spreading, and cytosqueletal organization, J. Biomed. Mater. Res. 241 (1998) 422–430.
[45] Y.-Y. Song, H. Hildebrand, P. Schmuki, Optimized monolayer grafting of 3-aminopropyltriethoxysilane onto amorphous, anatase and rutile TiO_2, Surf. Sci. 604 (3–4) (2010) 346–353.
[46] C.J. Da Costa Fernandes, F.J.B. Bezerra, B. De Campos Souza, M.A. Campos, W.F. Zambuzzi, Titanium-enriched medium drives low profile of ECM remodeling as a pre-requisite to pre-osteoblast viability and proliferative phenotype, J. Trace Elem. Med. Biol. 50 (2018) 339–346.
[47] M.H. Ginsberg, Integrin activation, BMB Rep. 47 (2014) 655–659.
[48] F. López-Huerta, et al., Biocompatibility and surface properties of TiO_2 thin films deposited by DC magnetron sputtering, Materials 7 (6) (2014) 4105–4117.

[49] S. Sangeetha, et al., Biocompatibility studies on TiO_2 coated Ti surface. 2013 International Conference on advanced nanomaterials and emerging engineering technologies (ICANMEET). Anais, 2013 International Conference on Advanced Nanomaterials and Emerging Engineering Technologies (ICANMEET) (2013).
[50] A. Huttenlocher, A.R. Horwitz, Integrins in cell migration, Cold Spring Harb. Perspect. Biol. 3 (2011) 1–16.
[51] F.G. Giancotti, E. Ruoslahti, Integrin signaling, Science 285 (1999) 1028–1032.
[52] W.F. Zambuzzi, et al., Ascorbate-induced osteoblast differentiation recruits distinct MMP-inhibitors: RECK and TIMP-2, Mol. Cell. Biochem. 322 (2009) 143–150.
[53] Zambuzzi Wf, R. Milani, A. Teti, Expanding the role of Src and protein-tyrosine phosphatases balance in modulating osteoblast metabolism: lessons from mice, Biochimie 92 (4) (2010) 327–332.
[54] W.F. Zambuzzi, J.M. Granjeiro, K. Parikh, S. Yuvaraj, M.P. Peppelenbosch, C.V. Ferreira, Modulation of Src activity by low molecular weight protein tyrosine phosphatase during osteoblast differentiation, Cell. Physiol. Biochem. 22 (5-6) (2008) 497–506.
[55] C.J.C. Fernandes, F. Bezerra, M.R. Ferreira, A.F.C. Andrade, T.S. Pinto, W.F. Zambuzzi, Nano hydroxyapatite-blasted titanium surface creates a biointerface able to govern Src-dependent osteoblast metabolism as prerequisite to ECM remodeling, Colloids Surf. B Biointerfaces 163 (2018) 321–328.
[56] M. Issler, A. Gomes, M. Rodrigues Ferreira, T. Silva Pinto, C. Fernandes, F. Bezerra, W. Zambuzzi, Cobalt-chromium-enriched medium ameliorates shear-stressed endothelial cell performance, J. Trace Elem. Med. Biol. 54 (2019) 163–171.
[57] D. Vanhoutte, et al., Relevance of matrix metalloproteinases and their inhibitors after myocardial infarction: a temporal and spatial window, Cardiovascular Res. 69 (3) (2006) 604–613.
[58] K. Kupai, et al., Matrix metalloproteinase activity assays: importance of zymography, J. Pharmacol. Toxicol. Methods 61 (2) (2010) 205–209.
[59] A. Mizutani, I. Sugiyama, E. Kuno, S. Matsunaga, N. Tsukagoshi, Expression of matrix metalloproteinases during ascorbateinduced differentiation of osteoblastic MC3T3-E1 cells, J. Bone Miner. Res. 16 (11) (2001) 2043–2049.